CrossMark

RESEARCH PAPER

Electrospinnability of Poly Lactic-co-glycolic Acid (PLGA): the Role of Solvent Type and Solvent Composition

Xiaoli Liu [1] · Stefania G. Baldursdottir [1] · Johanna Aho [1] · Haiyan Qu [2] · Lars Porskjær Christensen [2] ·
Jukka Rantanen [1] · Mingshi Yang [1,3]

ABSTRACT

Purpose In this study, the electrospinnability of poly(lactic-co-glycolic acid) (PLGA) solutions was investigated, with a focus on understanding the influence of molecular weight of PLGA, solvent type and solvent composition on the physical properties of electrospun nanofibers.

Method Various solvents were tested to dissolve two PLGA grades (50 KDa-RG755, 100 KDa-RG750). The viscoelasticity, surface tension, and evaporation rate of the PLGA solutions were characterized prior to the electrospinning process. The resulting electrospun nanofibers were characterized with respect to the morphology and mechanical properties.

Results Two pairs of solvent mixtures, i.e. dimethylformamide (DMF)—tetrahydrofuran (THF) and DMF—chloroform (CHL), were identified to provide a stable cone-jet. Within the polymer concentration range studied (10–30%, w/v), RG750 solutions could be electrospun into uniform fibers at 30% (w/v) or at 20% (w/v) when modifying the solvent composition. In comparison to DMF-THF solution, fibers had larger diameter, higher stiffness and tensile strength when electrospun from DMF-CHL solution.

Conclusion The high molecular weight polymer could ensure sufficient intermolecular interaction to generate uniform fibers. The solvent could influence the morphology and mechanical properties of the electrospun fibers by altering the properties of PLGA solution, and drying rate of fibers in the electrospinning process.

ABBREVIATIONS

$[\eta]$	Intrinsic viscosity
C^*	Overlap concentration
CHL	Chloroform
DMF	Dimethylformamide
ECM	Extracellular matrix
G'	Storage modulus
G''	Loss modulus
GA	Glycolic acid
LA	Lactic acid
LVR	Linear viscoelastic region
M_c	Critical molecular weight
MW	Molecular weight
PEG	Polyethylene glycol
PEO	Polyethylene oxide
PET-co-PEI	Poly(ethylene terephthalate-co-ethylene isophthalate)
PGA	Polyglycolic acid
PLA	Polylactic acid
PLGA	Poly(lactic-co-glycolic acid)
R_{coil}	Polymer coil radius
SEM	Scanning electron microscope
t	Time of flow of the polymer solution
t_0	Time of flow of the solvent solution
TGA	Thermogravimetric analysis
THF	Tetrahydrofuran
η_{rel}	Relative viscosity
η_{sp}	Specific viscosity

✉ Mingshi Yang
  mingshi.yang@sund.ku.dk

[1] Department of Pharmacy, University of Copenhagen, Universitetsparken 2, DK-2100 Copenhagen, Denmark

[2] Department of Chemical Engineering, Biotechnology and Environmental Technology, University of Southern Denmark, Campusvej 55, DK-5230 Odense, Denmark

[3] Wuya College of Innovation, Shenyang Pharmaceutical University, Wenhua Road No. 103, 110016 Shenyang, China

INTRODUCTION

Electrospinning has been widely investigated for producing scaffolds for tissue engineering (1–3), drug delivery systems (4,5), wound dressings (6,7), artificial organs (8) and vascular grafts (9). It is a versatile, cost effective, and simple process for making micro- or nanoscale fibers by exposing polymer solution/melt to a high voltage (10). As the voltage increases to break the balance between Coulombic repulsion and surface tension, a stable liquid jet can be discharged from the tip of the Taylor cone (11). With sufficient chain overlap and entanglements of the polymer molecules in the solution, and with a lateral electric force, a whip-like motion of the liquid jet between the capillary tip and the grounded collector is formed, and this motion results in thinning of the jet and formation of micro- or nanoscale fibers.

The electrospun fibers have been found to be a good mimic for the structure of the extracellular matrix (ECM) of the body (1,12,13). The electrospun fibrous mats, with a high pore volume with variable pore sizes, can enhance cell differentiation, adhesion, and proliferation (14). Different materials, such as synthetic or naturally derived polymers, can be processed alone or in combinations to promote various biological or physicochemical properties, such as biodegradation, biocompatibility, mechanical strength, hydrophobicity, or hydrophilicity, needed for different application purposes (3,15). Many natural polymers are unelectrospinnable due to molecular weight or solubility issues, and lack of mechanical properties. Compared to natural polymers, synthetic polymers have broader variation in physicochemical properties, and they are widely used in electrospinning.

In the electrospinning process, solution properties have a critical influence on the formation of the fibers (16). The most influential factors are solution viscosity, surface tension, and the net charge density carried by the electrospinning jet. High enough concentration of the polymer leads to entanglements, which has been found to be an essential prerequisite for the electrospinning process (10,16,17). However, too high concentration, and therefore, too high viscosity, prevents the polymer motion induced by the electric field. A decrease in the concentration below a threshold value changes the morphology of the produced samples from uniform fibers to beads. High surface tension has been shown to result in beaded fibers, whereas high viscosity and high net charge density, favor fibers with fewer beads. More charged solution, which can be created for example by adding ionic surfactant or salt to polymer solutions, can reduce the formation of beads and help in creating uniform fibers (2,18,19).

The viscosity of a polymer solution depends on molecular weight, molecular weight distribution, and molecular architecture of the polymer, as well as polymer concentration and solvent properties (20–22). With an increase in polymer concentration, the entanglement concentration can be reached, where the polymer chains overlap with one another that the individual chain motion is constrained. When the molecular weight exceeds the critical molecular weight (M_c), the intermolecular polymer chain interactions begin to dominate the flow behavior of the solution (23).

Recently, rheological properties of polymer solutions have been investigated to establish a link between their viscoelasticity and electrospinnability (17,24–26). A correlation between morphology of fibers and the rheological properties, such as chain entanglement and relaxation time, has been reported. Previous study showed that for a series of poly(ethylene terephthalate-co-ethylene isophthalate) (PET-co-PEI) copolymers, the polymer concentration must be at least 2–2.5 times higher than entanglement concentration in order to produce electrospun fibers (27). For different polymers, the requirement of the concentration can be different: For starch, the concentration had to be 1.2–2.7 times higher than the entanglement concentration in order to obtain fibers (17). However, another study, where polyethylene oxide (PEO) / polyethylene glycol (PEG) was studied, showed that the presence of entanglements was not a requisite for the formation of uniform fibers, and there was no correlation between the viscosity of the fluid and the fiber morphology: In fact it was the fluid elasticity controlling the morphology of the fibers produced by electrospinning (28). Despite that the viscoelasticity of polymer solutions is known to be critical for the electrospinning process, its impact on the electrospinnability and fiber characteristics are still not fully understood.

Poly lactic-co-glycolic acid (PLGA) has been widely investigated for medical uses, such as suture materials, bone fixation, implants, prosthetic devices, surgical sealant films and depot drug delivery systems (29,30). Recently electrospun PLGA nano- and microfibers have also been studied for bone regeneration, wound dressing, and tissue engineering (2,30,31). Besides its biodegradability and biocompatibility, the reason why this polymer is particularly attractive is the potential for controlled drug release (32,33). Although numerous studies have utilized PLGA to prepare electrospun nano- and microfibers for controlled-release purpose, not much is known about how the polymer solution properties influence the quality of electrospun PLGA fibers. To the best of our knowledge, this is the first study on how the viscoelasticity of PLGA solution influences its electrospinnability, and how the solvent type and solvent compositions influence the physical properties of electrospun nanofibers.

MATERIALS AND METHODS

Materials

PLGA (LA: GA, 75:25, molar ratio) with inherent viscosity (25°C, 0.1% chloroform [CHL]) in the range 0.50–0.70 dl/

g (RG755, MW 50,000–70,000 g/mol) and 0.8–1.2 dl/g (RG750, MW 120,000–190,000 g/mol) were purchased from Evonik (Darmstadt, Germany). Molecular biology grade N, N-dimethylformamide (DMF), HPLC grade tetrahydrofuran (THF), and CHL were obtained from Sigma-Aldrich (Denmark). All materials were used as obtained.

Preparation of Electrospun PLGA Nanofibers

The solvents including THF, DMF, CHL and their combinations were used in this study. The physical-chemical properties of the solvents are shown in Table. 1.

PLGA was dissolved in DMF-THF or DMF-CHL (40:60, 50:50, 60:40 v:v) at concentrations of 10%, 20%, and 30% (w/v), respectively. Electrospinning was conducted with our own customized setup, composed of a syringe pump (Harvard Apparatus), a 16 gauge needle (inner diameter 1.19 mm and outer diameter 1.65 mm), a custom-built high-voltage (20 kV max.) supply (PS/FC20R06, Glassman High Voltage Inc., USA), and a stationary plate for sample collection (Fig. 1). The electrospun samples was prepared at a flow rate of 10 μL/min, the distance between the nozzle tip to the grounded collector was 10 cm, and the voltage was adjusted to get a stable cone-jet. A rotating drum (1500 rpm) was used to collect the aligned fibers for tensile strength test.

Morphology of Electrospun Samples

The morphology and diameter of the electrospun samples were characterized using scanning electron microscope (SEM, Hitachi High-Tech HITACHI, USA). The samples were mounted on metal stubs with double-sided adhesive tape and coated under vacuum with gold in an argon atmosphere prior to observation. The specimens were then imaged at an accelerating voltage of 5 kV. The diameter distribution of electrospun fibers was determined by measuring around 200 fibers from the SEM images using the instrument software.

Table I   The Physical-Chemical Properties of the Solvents and Polymer

Solvent	Boiling point (°C)	Conductivity (m*K)	Evaporation rate (relative rate, butyl acetate = 1)	Surface tension (298.15 K) (mN/m)	Hildebrand solubility parameter ($MPa^{1/2}$)
THF	66	0.15	6.3	26.68	18.5
CHL	61	0.11	11.6	26.56	18.7
DMF	153	0.18	0.17	36.76	24.7
PLGA	–	–	–	–	~20

The Hildebrand solubility parameter of PLGA is obtained from previous publications (34)
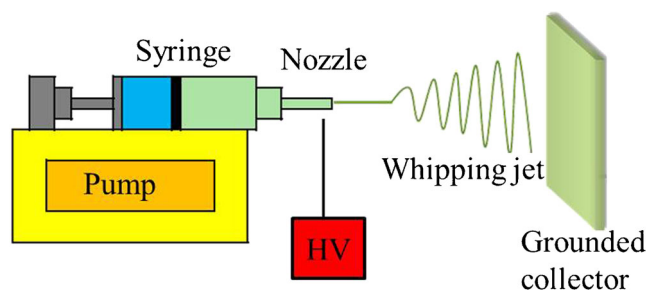
Fig. 1 Schematic illustration of a typical electrospinning setup.

Measurement of Intrinsic Viscosity

Viscosity measurements of the polymer solutions were measured using an Ubbelohde Semi-Micro dilution viscometer [No. 50, N213, CANNON Instrument Company, USA] at $25 \pm 0.2°C$, as described in a previous study (34). The viscosities were measured in dilute solutions (0.5%, 1%, 2%, 3%, w/v). The time of flow (t) was measured for each solution. The relative viscosity ($\eta_{rel} = t/t_0$) was calculated from the time of flow of the polymer solution (t) and that of the pure solvent (t_0). Specific viscosity was obtained from the equation $\eta_{sp} = \eta_{rel} -1$ (35). Subsequently, the reduced viscosity (η_{sp}/C) was calculated, where C is the polymer concentration in g/mL. The intrinsic viscosity ([η]) was obtained after extrapolation of η_{sp}/C as a function of C (Huggins plot), to a polymer concentration of zero. Also the overlap concentration (C*) for the two different PLGAs in different solvents were calculated according to equation $C* = 1/[\eta]$.

Oscillatory Shear and Steady Shear Measurements

The viscoelastic properties of PLGA solutions at varied concentrations were investigated using the DHR-3 Rheometer (TA Instruments, New Castle, DE, USA). All samples were analyzed on DHR-3 using the cone plate geometry (diameter = 40 mm, 1° cone angle) at 10°C, using a solvent trap to create a thermally stable vapour barrier to eliminate any solvent loss during rheological experiments. Oscillatory amplitude sweep tests were conducted to determine the linear viscoelastic region of each solution. Subsequently, oscillatory frequency sweeps from 0.1 to 100 rad/s were performed at the strain amplitude within the linear viscoelastic region. The shear viscosity of the solutions was investigated through a logarithmic steady shear rate increase from 0.1 to 1000 s^{-1}.

Measurement of Surface Tension

The surface tension of the polymer solutions was measured by pendant drop method using a KRUSS Drop Shape Analyzer—DSA100 (Hamburg, Germany). A drop of the measured solution was suspended in the air from a

needle of a syringe. The needle was inserted into a transparent glass box which has been saturated with the same solvent as the one dissolving the polymer at room temperature (22–23°C). The shape of the drop results from the interplay between the surface tension and gravity. In the pendant drop method, the surface tension is calculated from the shadow image of a pendant drop using drop shape analysis.

Measurement of Evaporation Rate

The evaporation rate of the solvents and polymer solutions was estimated by thermogravimetric analysis (TGA) (Discovery TGA, TA instruments, USA). Approximately 50 µL solvent or solution was transferred into a pre-tared platinum pan, and then enclosed inside the temperature controlled furnace and constantly purged with nitrogen gas at a flow rate of 10 mL/min. The temperature was kept constant at 25°C, because the electrospinning process was operated at room temperature. The weight loss was recorded as a function of time.

Measurement of Tensile Strength

The tensile strength measurements were carried out by TA.XT plus texture analyzer (Stable Micro Systems LTD., UK), equipped with a load cell which had a maximum load of 50N and a resolution of 1N. The test speed was 0.04 mm/s and the gripping distance was 40 mm. In order to avoid breakage of the sample during the sample fixing, the fibers were inserted into the gripping part together with an aluminum foil, which was cut before the measurement. A schematic diagram of the measurement is illustrated in Fig. 2.
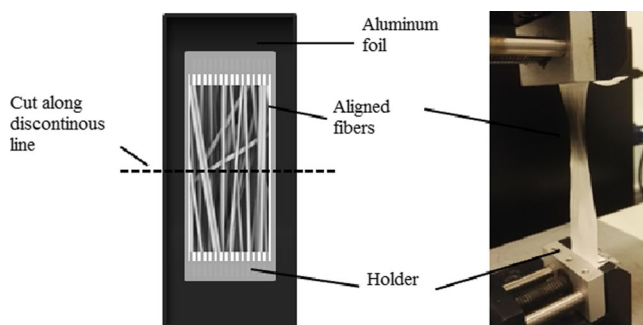
Fig. 2 Method used for the tensile strength test. The electrospun fibers along with aluminum foil were fixed between the grips of the texture analyzer. The aluminum foil was cut along the discontinuous line as shown, so that the load was experienced only by the fibers.

RESULTS

Intrinsic Viscosity

The intrinsic viscosities of RG755 and RG750 in different solvents are presented in Table 2. The intrinsic viscosity of RG750 was higher than RG755. Comparing the solvents THF and CHL, higher intrinsic viscosity can be observed when using CHL to dissolve the polymers. This can be related to a higher affinity of the polymer towards CHL, in which the polymer molecules are more extended and thus occupying a larger relative volume, represented by polymer coil radius, R_{coil}. As a result, the overlap concentration is lower.

Rheological Analysis of PLGA Solutions

Oscillatory Strain Sweep Measurements

Dynamic oscillatory sweep tests can provide useful information of the storage (elastic) and loss (viscous) moduli of PLGA solutions in response to the applied shear strain. The linear viscoelastic region (LVR) of the polymer solutions was identified by observing upper limit of strain where the loss and storage moduli are independent of the applied strain amplitude (Fig. 3). The LVR for both RG755 and RG750 grades varied for different solutions, being in the range from 1 to 100% for all the polymer solutions (≥20%, w/v). In addition, the polymer solutions showed a concentration dependent loss modulus, independent of the strain, which increased approximately by an order of magnitude with every 10% (w/v) increase in PLGA concentration. High strains resulted in a deviation from the linear region, indicated by a decrease in storage modulus (G′). Neither for RG755 nor for RG750, the LVR could be identified at low concentrations (<10% (w/v)) due to weak elastic moduli of the solutions. About an order of magnitude higher loss and storage moduli were observed for RG750 than for RG755 due to the

Table 2 The Polymer Behavior of RG755 and RG750 Solutions in Different Solvents

Polymer	Solvent	Solution parameters		
		Intrinsic viscosity ([η], dL/g)	Overlap Conc. (C*, %)	R_{coil} (nm)
RG755	THF	3.95	25.31	3.18
RG755	CHL	4.16	24.06	3.23
RG750	THF	7.29	13.71	5.15
RG750	CHL	9.22	9.22	5.57

Fig. 3 Oscillation strain sweep results of PLGA solutions at varying concentration. For each solution the storage modulus (G′) and loss modulus (G″) is represented by filled and open markers, respectively.
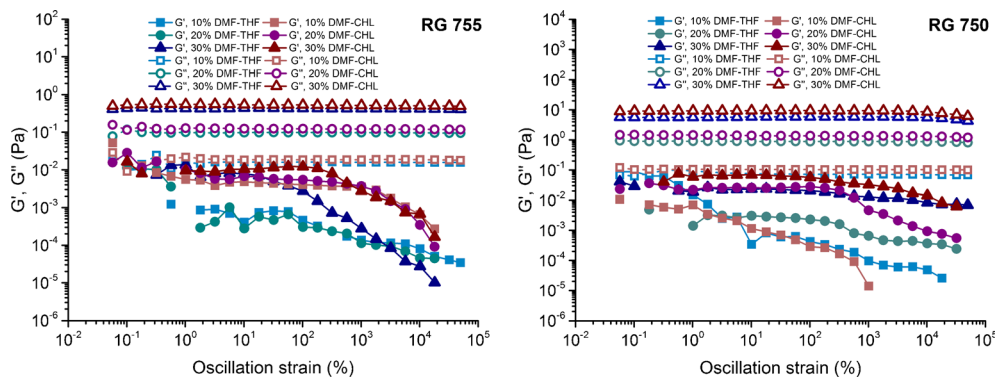
Fig. 4 Oscillation strain sweep results of PLGA solutions at varying solvent composition. For each solution the storage modulus (G′) and loss modulus (G″) is represented by filled and open markers, respectively.
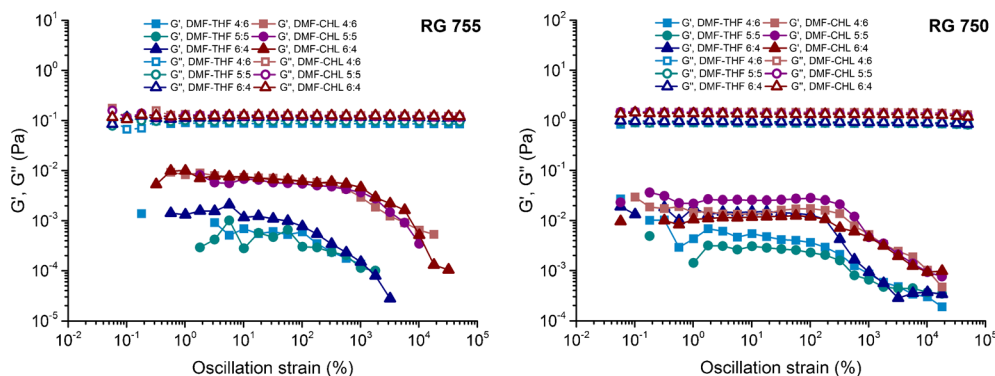
higher molecular weight of the polymer which results in more inter-molecular interaction and entanglements.

When changing the composition ratio of the solvents, the loss modulus remained nearly unchanged, as shown in Fig. 4. PLGA dissolved in DMF-CHL had a higher G′ than that in DMF-THF. However, the ratios of the solvents in the mixture did not influence the linear viscoelastic region.

Oscillatory Frequency Sweep Measurements

Both RG755 and RG750 solutions showed a significant increase in loss modulus (G″) in response to an increase in frequency at 5% strain with a typical concentration dependence

(Fig. 5). All the solutions were predominantly viscous, G″ being significantly higher than storage modulus (G′). A slightly higher G″ can be seen for PLGA solutions in DMF-CHL compared to DMF-THF at the same concentration. The solvent composition did not influence G″, whereas G′ had a slightly different pattern (Fig. 6). G′ showed higher values when the polymer was dissolved in DMF-CHL than in DMF-THF. This indicates a more elastic behavior of the DMF-CHL polymer solution: the intermolecular chain interactions force the polymer to recover to its original shape after removing external force. The G′ showed a plateau at low frequency range, similar to what may be observed for structured and heterogeneous fluids.


Fig. 5 Oscillation frequency sweep results of PLGA polymer solutions at varying concentration. For each solution the storage modulus (G′) and loss modulus (G″) is represented by filled and open markers, respectively.
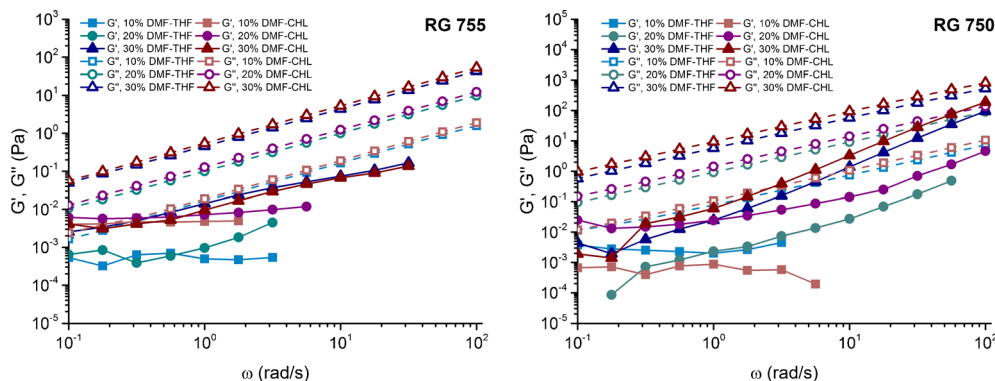
Fig. 6 Oscillation frequency sweep results of PLGA polymer solutions at varying solvent composition. For each solution the storage modulus (G′) and loss modulus (G″) is represented by filled and open markers, respectively. The values below 10^{-4} Pa are close the torque detection limit.
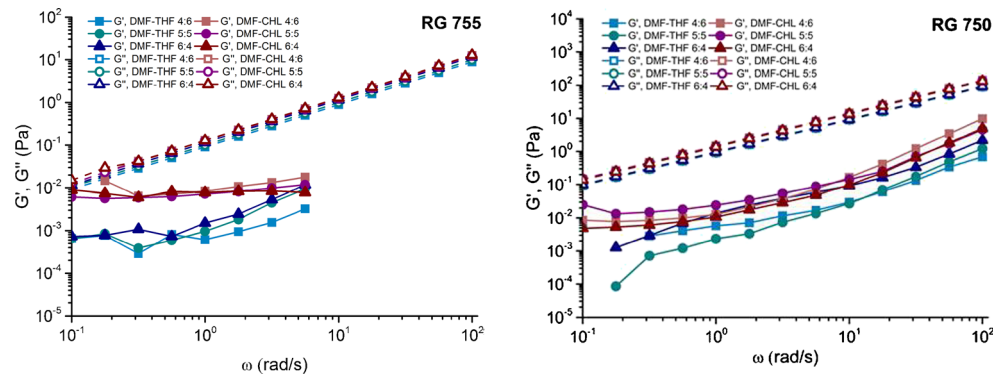
Fig. 7 Shear viscosity of PLGA polymer solutions at varying concentration.
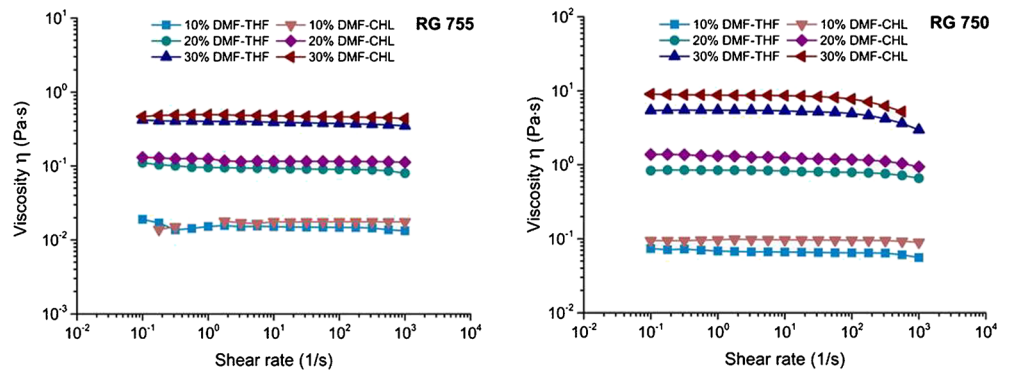
Shear Viscosity of PLGA Solutions

As expected, the shear viscosity got higher as the polymer concentration and the molecular weight were increased (Fig. 7). RG750 exhibited non-Newtonian behavior when the shear rate was above 100 s^{-1}. Shear thinning of high molecular weight polymer solutions, is attributed to shear induced changes in molecular interactions, namely molecular disentanglement and orientation with the flow direction. In general, the polymers dissolved in DMF-CHL showed slightly higher viscosity than that dissolved in DMF-THF.

The shear viscosity of RG755 and RG750 solutions was found to be independent of the composition of the dual-solvent systems (Fig. 8). Most of RG755 solutions, when dissolved in

DMF-CHL, showed an initial drop in shear viscosity at the low shear rates, while for RG750 the ratio between the initial and plateau values was lower and thus not readily observable in Fig. 8. This kind of behavior is often observed in fluids which show apparent yield stress (36). When the plateau was reached with an increase in the shear stress (shear rate), the shear viscosity of polymer solutions was only solvent dependent, and independent of the solvent compositions in the range studied.
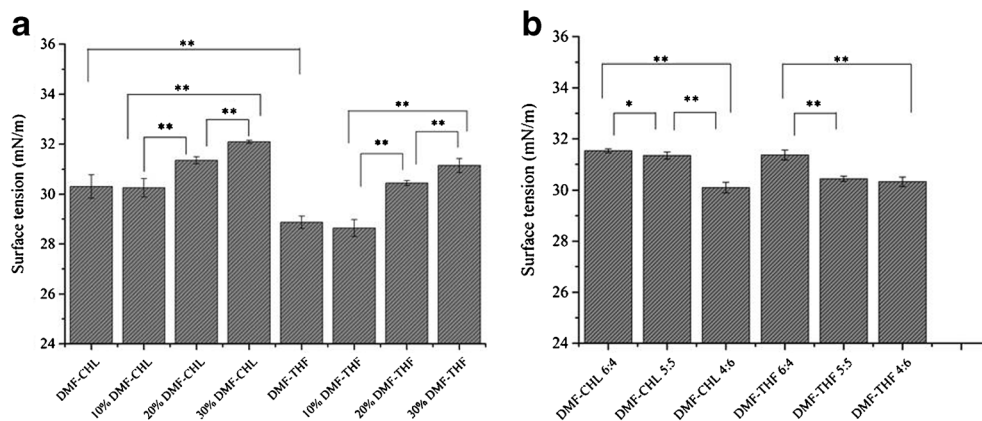
Surface Tension of PLGA Solutions

The results from the pendant drop method showed that the surface tension of polymer solutions was significantly increased with an increase in polymer concentration

Fig. 8 Shear viscosity of PLGA polymer solutions at different solvent compositions.
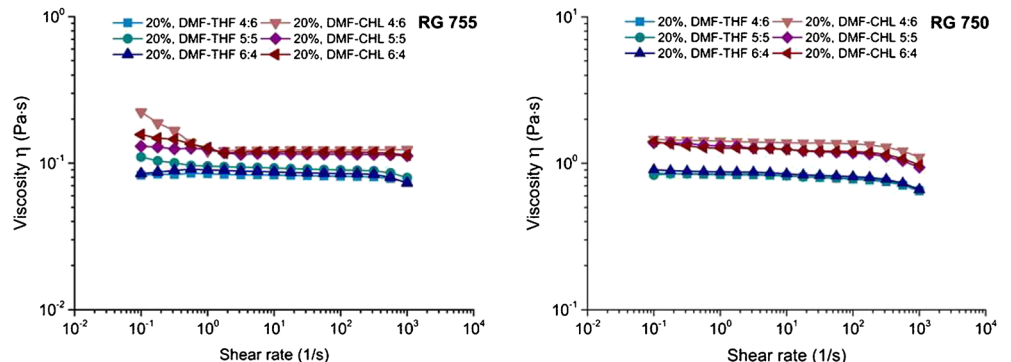
Fig. 9 The surface tension of different polymer solutions. $**p < 0.01$, $*p < 0.05$. (**a**) polymer solutions at different concentration; (**b**) polymer solutions in different solvent compositions at the same concentration (20% w/v).
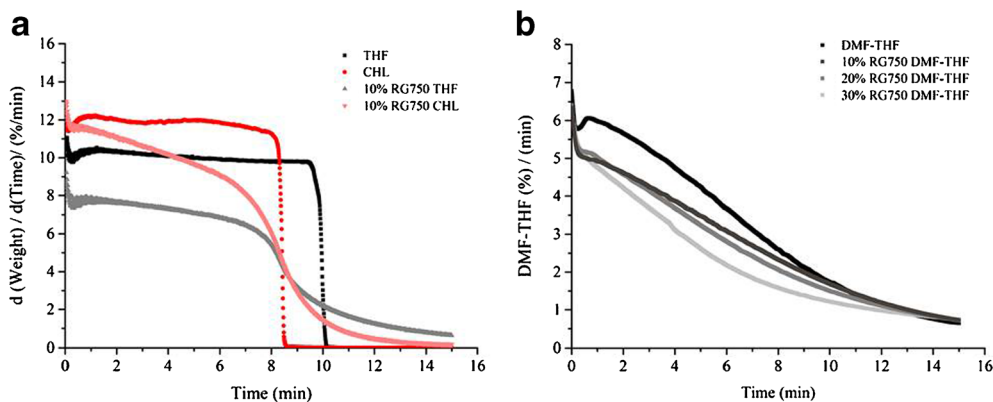

(Fig. 9a). At the same polymer concentration, the surface tension of PLGA solutions was also increased with an increase in the proportion of DMF, because DMF has a higher initial surface tension than THF and CHL as shown in Table 1 (Fig. 9b). The difference between solvents DMF-CHL and DMF-THF was also obvious; all the polymer solutions dissolved in DMF-CHL had a significantly higher surface tension than the ones dissolved in DMF-THF (** was only shown between DMF-CHL and DMF-THF, but the difference is also significant between the polymer solutions in different solvents at the same concentration, in Fig. 9a).

Evaporation Rate of PLGA Solutions

In Fig. 10a, the evaporation rates of THF and CHL, and of 10% (w/v) PLGA 750 dissolved in these two solvents are depicted, while Fig. 10b shows the evaporation rates of DMF-THF and of RG750 dissolved in it at different concentrations. The results showed that the evaporation rates of pure solvents were constant, but became slower in polymer solutions as the polymer concentration was increased with an evaporation of the solvents. Figure 10b also shows that the solvent evaporation rates decreased slightly with an increase in the polymer concentration.

Morphology of Electrospun Samples

The voltages used in the electrospinning process in this study are summarized in Table 3. The voltage was adjusted to maintain a stable cone-jet, yet varying it as little as possible. The status of the cone-jet is described in the table. As observed in the study, discontinuous streams appeared when the proportion of DMF in the solvent composition was decreased: The cone-jet was more stable with an increase in DMF proportion or polymer concentration.

The morphology of electrospun PLGA samples changed from monodispersed particles to beaded fibers for RG755, and from beaded fibers to spindle fibers and then uniform fibers for RG750, regardless of whether DMF-THF or DMF-CHL was used as a co-solvent (Figs. 11 and 12). However, the surface of the samples prepared from DMF-THF system seemed to be smoother compared to that from DMF-CHL. The diameter of the fibers from DMF-CHL was larger and more uniform than that from DMF-THF (Fig. 13).

The solvent composition seemed to affect the morphology of the electrospun samples. As shown in Fig. 14, samples changed from beaded fibers to almost multi-dispersed particles for RG755 (Fig. 14a–d) with an increase in DMF proportion from 40 to 60% (v/v), whereas for RG750 (Fig. 14e–h), the fibers changed from uniform fibers to spindle fibers. This is

Fig. 10 Evaporation rate of different solvents and polymer solutions. (**a**) pure solvents and polymer solutions dissolved in the same solvent; (**b**) polymer solutions at different concentration.

Table 3 Polymer Solution Compositions and Parameters Used in the Electrospinning Process

Polymer	Concentration (w/v%)	DMF-THF (v:v)	Voltage (Kv)	Cone-jet	DMF-CHL (v:v)	Voltage (Kv)	Cone-jet
RG755	10%	5:5	9.0	Stable	5:5	8.5	Stable
RG755	20%	4:6	9.0	Stable	4:6	8.5	Stable
RG755	20%	5:5	9.0	Stable	5:5	8.5	Stable
RG755	20%	6:4	8.5	Stable	6:4	8.5	Stable
RG755	30%	5:5	9.0	Stable	5:5	8.5	Stable
RG750	10%	5:5	8.0	Stable	5:5	8.0	Stable
RG750	20%	4:6	7.0/ 8.0/ 9.0	Discontinuous stream	4:6	7.0/ 8.0/ 9.0	Discontinuous stream
RG750	20%	5:5	7.0/ 8.0/ 9.0	Discontinuous stream	5:5	8.0	Stable
RG750	20%	6:4	8.0	Stable	6:4	8.0	Stable
RG750	30%	5:5	8.0	Stable	5:5	8.0	Stable

a result of increased surface tension, decreased evaporation rate, and nearly unchanged viscosity.

Tensile Strength

The electrospun samples prepared from 30% (w/v) RG750 solutions were selected and tested in this study. As shown in Fig. 15, the initial part of the stress–strain curve exhibits the typical elastic behavior. Young's modulus, which represents the stiffness of the material, is calculated from the initial, linear part of the curve. The fibers prepared from DMF-CHL showed a higher Young's modulus of 673 ± 43 MPa, compared with 438 ± 61 MPa of the fibers prepared from DMF-THF. A yield point is then observed after the initial linear region. The slope of stress–strain curve began to decline

gradually due to the fiber slippage. Further increases in strain lead to a well-defined failure of the electrospun fibers. The fibers prepared from DMF-CHL exhibited higher yield strength and ultimate tensile strength as compared to the fibers prepared from solvent DMF-THF.

DISCUSSION

Effect of Molecular Weight on the Electrospinnability

According to the generalized Maxwell model for entangled polymers, the G' curve in the lower frequency range should show a slope of 2:1 (log-log scale) and G'' curve should have a slope of 1:1 (37,38). From our results, only RG750 at 30%

Fig. 11 The morphology of electrospun samples of PLGA solutions at varied concentration in DMF-THF. (**a**, **b**, **c**) are RG755 at concentration of 10%, 20%, and 30% w/v; (**d**, **e**, **f**) are RG750 at concentration of 10%, 20%, and 30% w/v. The inset image in the upper-left corner is the magnification of the same sample.
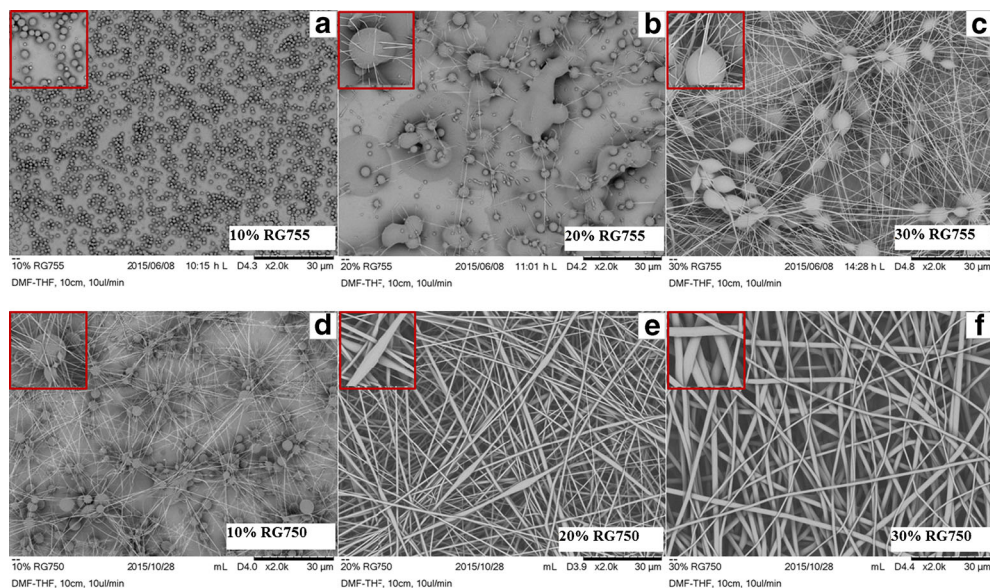
Fig. 12 The morphology of electrospun samples of PLGA solutions at varied concentration in DMF-CHL. (**a**, **b**, **c**) are RG755 at concentration of 10%, 20%, and 30% w/v; (**d**, **e**, **f**) are RG750 at concentration of 10%, 20%, 30% w/v. The inset image in the upper-left corner is the magnification of the same sample.
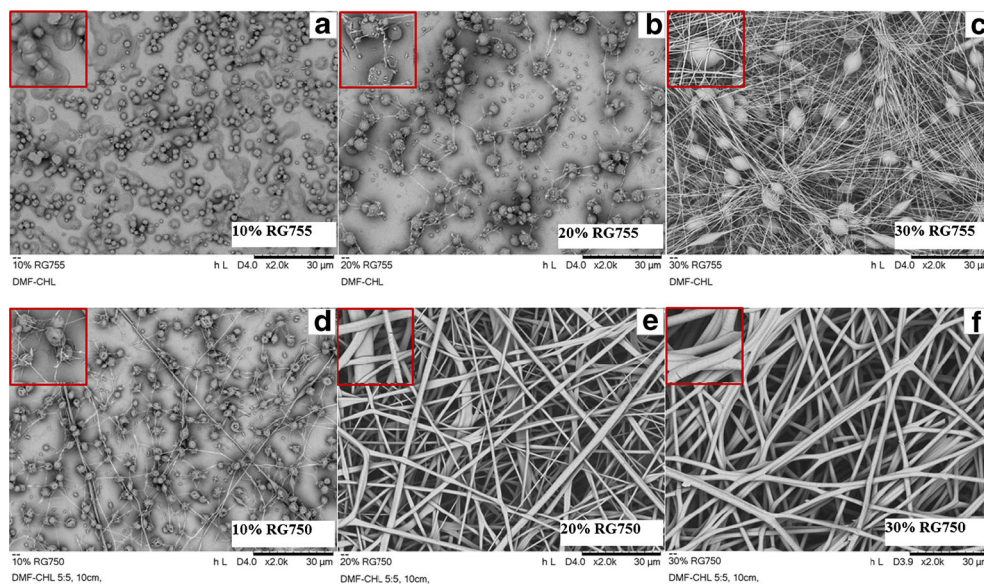
(w/v) concentration had this typical behavior. Referring to the study by Graessley (23), all RG755 solutions (from 10–30%, w/v) and RG750 solutions below 20% (w/v) are located in the semidilute but not entangled region. Our results are consistent with the theory, showing that the higher molecular weight RG750 at higher concentration could form uniform fibers.

Effect of Solvent Type on the Electrospinnability

The polymer dissolved in DMF-CHL has a slightly higher loss modulus G'' than that dissolved in DMF-THF, and as a result, the fibers with a larger diameter were produced. Generally, a higher G'' could be observed when polymer was dissolved in DMF-CHL, compared to DMF-THF. CHL seemed to be a better solvent than THF for both RG755 and RG750, as shown in the intrinsic viscosity data. This means that the
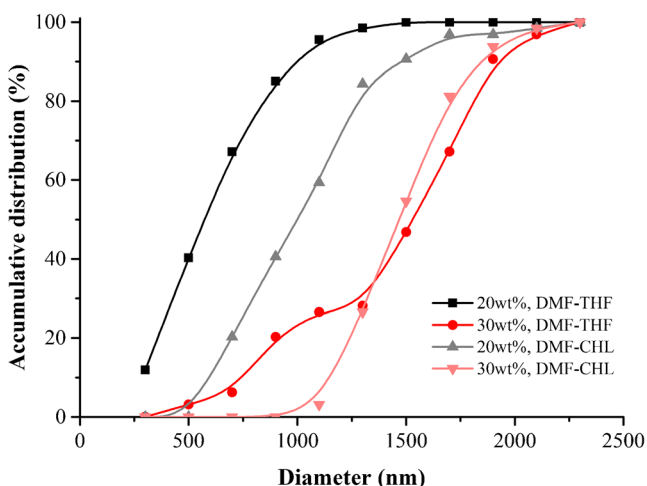

Fig. 13 The fiber diameter distribution of RG750 dissolved in different solvents at varied concentration

polymer molecules in DMF-CHL are more stretched and more overlapping at the same concentration. Therefore, the overlap concentration of polymer dissolved in DMF-CHL is lower than that dissolved in DMF-THF. As a result, the minimum electrospinnable polymer concentration was lower in CHL than in THF.

The difference in the morphology of the electrospun samples may be attributed to the different elasticity of polymer solutions. The polymer solutions dissolved in DMF-CHL exhibited higher G' than the solutions in DMF-THF, which may help creating a more stable extensional flow in the spinning process (39–41). Previous studies also showed that capillary forces can gradually squeeze the fluid into "beads" connected by highly elastic strings (28). If the instability of the electrospinning jet is completely suppressed by elastic forces or arrested at a very early stage of instability, the produced fibers will have a uniform appearance. In this study, the higher elasticity achieved by using DMF-CHL could suppress the bead formation and result in uniform fibers. In addition, the elasticity contributes to the recovery of the original conformation of the polymer molecules as the solvent evaporates.

Besides the diameter and morphology, the fibers generated from different solvent systems exhibited different mechanical properties. As mentioned above, entanglements were observed in the 30% RG750 polymer solution. During the electrospinning process, both the electric force and high surface tension tended to destroy the entanglements. When RG750 was dissolved in DMF-CHL, it had a higher viscosity, which means that it had higher intermolecular interaction to resist the change caused by the external force. Its higher elasticity means that it had a higher potential to recover to its original status after removal of the external force. As a result, the molecular entanglements were sustained after the
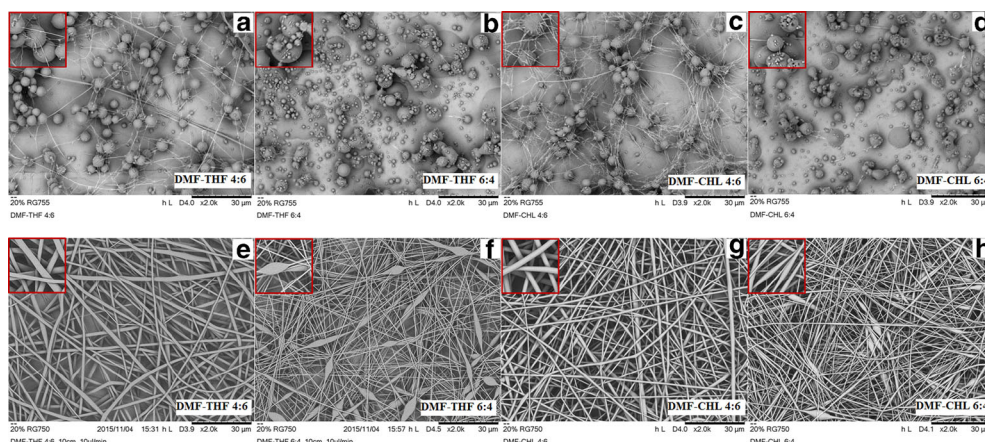
Fig. 14 The morphology of electrospun samples of PLGA solutions at 20 w/v% in varied compositions of the solvent system. (**a**) and (**b**) RG755 dissolved in varied composition of DMF-THF; (**c**) and (**d**) RG755 dissolved in varied composition of DMF-CHL. (**e**) and (**f**) RG750 dissolved in varied composition of DMF-THF; (**g**) and (**h**) RG750 dissolved in varied composition of DMF-CHL. The inset image in the upper-left corner is the magnification of the same sample.

Fig. 15 Tensile behavior of aligned fibers prepared from different solvents at 30% concentration. Three typical representative curves for each sample are presented.
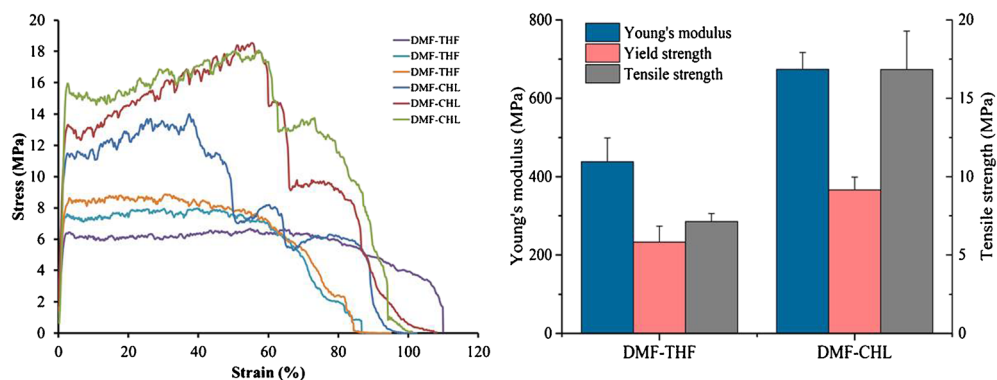

electrospinning process when using DMF-CHL as the solvent. Therefore, the dried fibers have more intermolecular network, which was preserved during the electrospinning process, resulting in a higher stiffness and tensile strength of the fibers.

Influence of Polymer Solution Properties on Electrospinnability and Fiber Properties

For both 20% (w/v) RG750 solution (DMF:THF/CHL, 4:6, v/v) and 30% (w/v) RG750 solution (DMF:THF/CHL, 5:5, v/v), uniform fibers could be produced. The influence of the viscosity and surface tension of feed solutions on the morphology of electrospun samples was plotted in Fig. 16 using the experimental data obtained in this study. The morphology of electrospun fibers can be divided into the following three types, particles (including particles with ultra-thin fibers), beaded fibers (thinner fibers with spherical beads), and fibers (including spindle fibers). In this study, the polymer solutions were unable to form fibers with a viscosity lower than around 0.8 Pa·s. With an increase in polymer concentration, both the viscosity and surface tension of the solutions were increased. However,

the viscosity plays a dominant role in determining whether fibers could be produced. At the same polymer concentration, a change in the solvent composition can result in a change of both viscosity and surface tension of the polymer solutions. When the viscosity of polymer solutions can
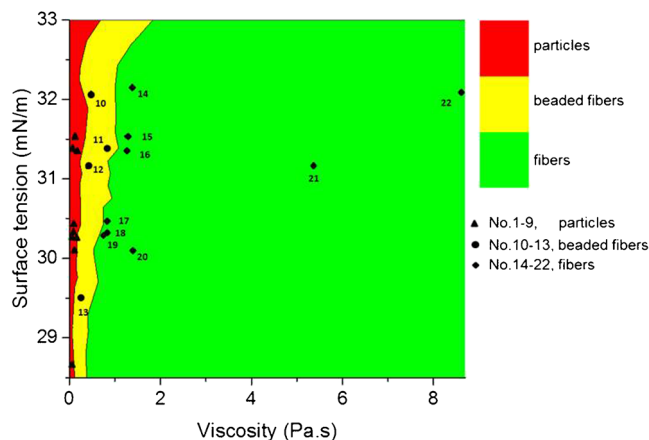
Fig. 16 The relationship between the morphology of electrospun samples as a function of the changing surface tension and viscosity of the polymer solutions. The black markers represent the data obtained in this study.

overpower the effect of the surface tension, uniform fibers can be produced. The morphology of the electrospun samples could be modified by changing the concentration of polymer solution and the composition of solvents.

A link between the mechanical properties of fibers and the rheological properties of polymer solutions seems to exist. The mechanical properties, such as Young's modulus and tensile strength, are in proportion with network or physical entanglement between polymer molecules. In this study, the mechanical properties of the fibers are affected by the network preservation of the molecular entanglement in the solutions after electrospinning.

CONCLUSION

Similar to other electrospinnable polymers, a high-molecular weight PLGA could be electrospun into uniform nanofibers when the polymer concentration was sufficiently high. This can be attributed to sufficient intermolecular interaction of the polymer in the electrospinning process, *i.e.* molecular entanglement. Nevertheless, the concentrated but not entangled PLGA solutions could also be electrospun into uniform fibers when the surface tension and viscoelasticity of polymer solution were appropriate, dictated by the solvent types and solvent compositions. Consequently, the morphology and mechanical properties of the electrospun PLGA fibers can be adjusted by the selection of the solvent types and solvent compositions. This study demonstrated that rheological characterization was a useful tool to gain insight into the PLGA fiber formation in the electrospinning process.

ACKNOWLEDGMENTS AND DISCLOSURES

REFERENCES

1. Dhandayuthapani B, Yoshida Y, Maekawa T, Kumar DS. Polymeric scaffolds in tissue engineering application: a review. Int J Polym Sci. 2011;2011:1–19.
2. Jose MV, Thomas V, Johnson KT, Dean DR, Nyairo E. Aligned PLGA/HA nanofibrous nanocomposite scaffolds for bone tissue engineering. Acta Biomater. 2009;5(1):305–15.
3. Cooper JA, Lu HH, Ko FK, Freeman JW, Laurencin CT. Fiber-based tissue-engineered scaffold for ligament replacement: design considerations and in vitro evaluation. Biomaterials. 2005;26(13): 1523–32.
4. Chou SF, Carson D, Woodrow KA. Current strategies for sustaining drug release from electrospun nanofibers. J Control Release. 2015;220(Pt B):584–91.
5. Goonoo N, Bhaw-Luximon A, Jhurry D. Drug loading and release from electrospun biodegradable nanofibers. J Biomed Nanotechnol. 2014;10(9):2173–99.
6. Boateng J, Catanzano O. Advanced therapeutic dressings for effective wound healing—a review. J Pharm Sci. 2015;104(11):3653–80.
7. Rieger KA, Birch NP, Schiffman JD. Designing electrospun nanofiber mats to promote wound healing—a review. J Mater Chem B. 2013;1(36):4531.
8. Szentivanyi AL, Zernetsch H, Menzel H, Glasmacher B. A review of developments in electrospinning technology: new opportunities for the design of artificial tissue structures. Int J Artif Organs. 2011;34(10):986–97.
9. Theron JP, Knoetze JH, Sanderson RD, Hunter R, Mequanint K, Franz T, *et al*. Modification, crosslinking and reactive electrospinning of a thermoplastic medical polyurethane for vascular graft applications. Acta Biomater. 2010;6(7):2434–47.
10. Bhardwaj N, Kundu SC. Electrospinning: a fascinating fiber fabrication technique. Biotechnol Adv. 2010;28(3):325–47.
11. Christanti Y, Walker LM. Surface tension driven jet break up of strain-hardening polymer solutions. J Non-Newtonian Fluid Mech. 2001;100(1):9–26.
12. Zhu X, Cui W, Li X, Jin Y. Electrospun fibrous mats with high porosity as potential scaffolds for skin tissue engineering. Biomacromolecules. 2008;9(7):1795–801.
13. Li WJ, Laurencin CT, Caterson EJ, Tuan RS, Ko FK. Electrospun nanofibrous structure: a novel scaffold for tissue engineering. J Biomed Mater Res. 2002;60(4):613–21.
14. Prabaharan M, Jayakumar R, Nair S. Biomedical applications of polymeric nanofibers. In: Springer; 2012.
15. Freyman T, Yannas I, Gibson L. Cellular materials as porous scaffolds for tissue engineering. Prog Mater Sci. 2001;46(3):273–82.
16. Shenoy SL, Bates WD, Frisch HL, Wnek GE. Role of chain entanglements on fiber formation during electrospinning of polymer solutions: good solvent, non-specific polymer–polymer interaction limit. Polymer. 2005;46(10):3372–84.
17. Kong L, Ziegler GR. Role of molecular entanglements in starch fiber formation by electrospinning. Biomacromolecules. 2012;13(8):2247–53.
18. Shin Y, Hohman M, Brenner M, Rutledge G. Experimental characterization of electrospinning: the electrically forced jet and instabilities. Polymer. 2001;42(25):09955–67.
19. McKee MG, Hunley MT, Layman JM, Long TE. Solution rheological behavior and electrospinning of cationic polyelectrolytes. Macromolecules. 2006;39(2):575–83.
20. Gandhi K, Williams MC. Solvent effects on the viscosity of moderately concentrated polymer solutions. In: Journal of Polymer Science Part C: Polymer Symposia: Wiley Online Library; 1971. p. 211–234.
21. Isono Y, Fujimoto T, Inagaki H, Shishido M, Nagasawa M. Viscoelastic properties of branched polymers. I. At the undiluted state. Polym J. 1980;12(2):131–7.
22. Isono Y, Fujimoto T, Kajiura H, Nagasawa M. Viscoelastic properties of branched polymers. II in concentrated solutions. Polym J. 1980;12(6):369–78.
23. Graessley WW. The entanglement concept in polymer rheology. In: The entanglement concept in polymer rheology. Springer; 1974. p. 1–179.
24. Kong L, Ziegler GR. Rheological aspects in fabricating pullulan fibers by electro-wet-spinning. Food Hydrocoll. 2014;38:220–6.
25. Kong L, Ziegler GR. Fabrication of pure starch fibers by electrospinning. Food Hydrocoll. 2014;36:20–5.

26. Klossner RR, Queen HA, Coughlin AJ, Krause WE. Correlation of chitosan's rheological properties and its ability to electrospin. Biomacromolecules. 2008;9(10):2947–53.

27. McKee MG, Wilkes GL, Colby RH, Long TE. Correlations of solution rheology with electrospun fiber formation of linear and branched polyesters. Macromolecules. 2004;37(5):1760–7.

28. Yu JH, Fridrikh SV, Rutledge GC. The role of elasticity in the formation of electrospun fibers. Polymer. 2006;47(13):4789–97.

29. Pandey A, Jain DS. Poly Lactic-Co-Glycolic Acid (PLGA) copolymer and its pharmaceutical application. Handbook of polymers for pharmaceutical technologies: processing and applications, volume 2. 2015.p. 151–172.

30. Singh G, Kaur T, Kaur R, Kaur A. Recent biomedical applications and patents on biodegradable polymer-PLGA. Int J Pharmacol Pharm Sci. 2014;1:30–42.

31. Chang N-J, Lam C-F, Lin C-C, Chen W-L, Li C-F, Lin Y-T, et al. Transplantation of autologous endothelial progenitor cells in porous PLGA scaffolds create a microenvironment for the regeneration of hyaline cartilage in rabbits. Osteoarthr Cartil. 2013;21(10):1613–22.

32. Sahoo S, Toh SL, Goh JC. A bFGF-releasing silk/PLGA-based biohybrid scaffold for ligament/tendon tissue engineering using mesenchymal progenitor cells. Biomaterials. 2010;31(11):2990–8.

33. Hong Y, Fujimoto K, Hashizume R, Guan J, Stankus JJ, Tobita K, et al. Generating elastic, biodegradable polyurethane/poly (lactide-co-glycolide) fibrous sheets with controlled antibiotic release via two-stream electrospinning. Biomacromolecules. 2008;9(4):1200–7.

34. Baldursdóttir SG, Kjøniksen A-L, Karlsen J, Nyström B, Roots J, Tønnesen HH. Riboflavin-photosensitized changes in aqueous solutions of alginate. Rheological studies. Biomacromolecules. 2003;4(2):429–36.

35. Gomes D, Borges C, Pinto J. Evaluation of parameter uncertainties during the determination of the intrinsic viscosity of polymer solutions. Polymer. 2000;41(14):5531–4.

36. Møller P, Fall A, Bonn D. Origin of apparent viscosity in yield stress fluids below yielding. EPL. 2009;87(3):38004.

37. Mezger TG. The rheology handbook: for users of rotational and oscillatory rheometers: Vincentz Network. 2006.

38. Morrison FA. Understanding rheology. USA: Oxford University Press; 2001.

39. Elliott PT, Steffenhagen MJ, Glass JE. Spray applications: Part III. Assessment of viscosities at high shear rates and dynamic uniaxial extensional viscosities on fan nozzle air sprayability. J Coat Technol Res. 2007;4(4):341–9.

40. Crooks R, Cooper-White J, Boger DV. The role of dynamic surface tension and elasticity on the dynamics of drop impact. Chem Eng Sci. 2001;56(19):5575–92.

41. Kennedy JC, Meadows J, Williams PA. Shear and extensional viscosity characteristics of a series of hydrophobically associating polyelectrolytes. J Chem Soc Faraday Trans. 1995;91(5):911–6.